

How to tap an innocent waveguide

Michael Paulus^{1,2} and Olivier J. F. Martin¹

¹ *Electromagnetic Fields and Microwave Electronics Laboratory
Swiss Federal Institute of Technology, ETH-Zentrum, ETZ
CH-8092 Zurich, Switzerland*

² *IBM Research, Zurich Research Laboratory
CH-8803 Rüschlikon, Switzerland*

*paulus@ifh.ee.ethz.ch, martin@ifh.ee.ethz.ch
<http://www.ifh.ee.ethz.ch/~martin>*

Abstract: We study the interaction of a mode propagating in a planar waveguide with a three-dimensional rectangular defect (protrusion or notch) in the structure. The scattering by the defect disturbs the propagation of the mode and light is coupled out of the waveguide. To investigate these phenomena we compute electric field distributions with the Green's tensor technique and show movies with varying defect geometries and different mode polarizations. These calculations should be useful for optimizing specific elements in complex photonic circuits.

© 2001 Optical Society of America

OCIS codes: (130.0130) Integrated optics; (230.0230) Optical devices; (260.3160) Interference; (260.5430) Polarization; (290.0290) Scattering.

References and links

1. R. G. Hunsperger, *Integrated Optics: Theory and Technology*, 3rd ed. (Springer, Berlin, 1991).
2. T. Tamir and S. T. Peng, "Analysis and Design of Grating Couplers," *Appl. Phys.* **14**, 235–254 (1977).
3. M. Paulus, P. Gay-Balmaz, and O. J. F. Martin, "Accurate and efficient computation of the Green's tensor for stratified media," *Phys. Rev. E* **62**, 5797–5807 (2000).
4. M. Paulus and O. J. F. Martin, "Light propagation and scattering in stratified media: A Green's tensor approach," *J. Opt. Soc. Am. A* **18**, 854–861 (2001).
5. D. Marcuse, *Light transmission optics*, 2nd ed. (Krieger, Malabar, 1989).
6. M. Born and E. Wolf, *Principles of Optics*, 6th. ed. (Pergamon Press, Oxford, 1987).

1 Introduction

In many applications the coupling of optical energy out of or into a waveguide is obtained by a grating deposited on top of the structure [1]. The properties of such a grating like the coupling efficiency and the angular distribution of the radiated electric field strongly depend on the shape, the size and the periodicity of the individual elements forming the grating [2]. For a quantitative analysis the collective behavior of these elements must be taken into account. However, from a physical point of view, much can be learned from the reduced problem of a "grating" with a single element.

In this paper we focus on the scattering by a three-dimensional (3D) rectangular defect in the planar InP/InGaAsP waveguide structure depicted in Fig. 1. The extension of the scattering element in the x and the y directions is $0.5 \times 0.5 \mu\text{m}^2$ and held fixed. We deliberately choose a defect smaller than the wavelength to avoid any resonance effects and concentrate our study on the influence of the vertical extension of the defect. In the z direction we vary the defect height between $h = 500 \text{ nm}$ and $h = -800 \text{ nm}$. For positive z values the defect forms a protrusion on the waveguide structure whereas

negative z values correspond to a notch etched into the waveguide. We show electric field distributions calculated by computer simulations and discuss the effects associated with the height variation for different polarizations of the waveguide mode.

2 Model

An accurate calculation of the scattered electric field requires the solution of the vectorial wave equation with boundary conditions given at the different material interfaces. In our case the entire structure is formed by the 3D scattering element (protrusion or notch) embedded in the planar stratified waveguide (see Fig. 1). We recently proposed an approach to this problem based on the Green's tensor technique [3, 4]. This fully vectorial model provides a self-consistent and accurate solution of the electric field integral equation. The advantage of this approach lies in the fact that the boundary conditions at the different material interfaces, as well as at the edges of the computation window are automatically and perfectly fulfilled and artificial absorbing boundary conditions are not needed. Further, only the protrusion/notch must be discretized, the remaining of the structure being accounted for in the Green's tensor. We refer the interested reader to Ref. [4], where the specificities of this approach are discussed in detail and compared to alternative techniques for computational optics.

3 Results

At a wavelength $\lambda = 1.55 \mu\text{m}$ the planar InP/InGaAsP waveguide supports a transverse electric mode (TE_0 , electric field polarized in the y direction) and a transverse magnetic mode (TM_0 , electric field polarized in the xz plane). The corresponding propagation constants are $\beta_{\text{TE}_0} = 12.96 \mu\text{m}^{-1}$ and $\beta_{\text{TM}_0} = 12.92 \mu\text{m}^{-1}$ [5]. For both modes we present movies of the electric field amplitude (square root of $\mathbf{E} \cdot \mathbf{E}^*$) as a function of the defect height h . When $h = 0$ the defect vanishes and the total electric field is simply given by the excitation in the stratified background. In all cases we assume that the incident mode propagates in the positive x direction.

The movies in Fig. 2 show side views of the electric field distribution, when a TE_0 mode is used as excitation. Obviously, the field remains fairly unaffected by a protrusion [$h > 0$, Fig. 2(a)]. On the other hand, with a notch building up ($h < 0$), the incident mode is reflected at the waveguide/air interface and an interference pattern caused by the interaction of the incident field with the reflected one appears on the left-hand side of the notch. In the forward direction the propagation of the mode is disrupted and the field amplitude is depleted just behind the defect. However, this depletion remains

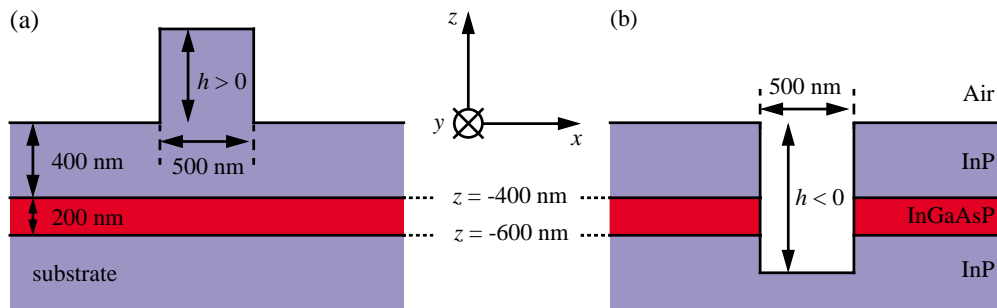


Fig. 1. Geometry of the investigated InP/InGaAsP planar waveguide structure (permittivities $\epsilon_{\text{InP}} = 10.05$, $\epsilon_{\text{InGaAsP}} = 11.42$, wavelength $\lambda = 1.55 \mu\text{m}$). Either (a) a protrusion with height $h > 0$ is deposited on or (b) a notch with depth $h < 0$ is etched through the structure. This scattering element has a finite lateral extension (500 nm) in both the x and the y directions.

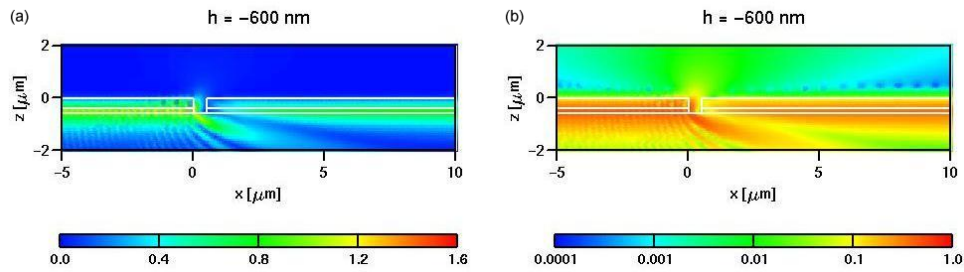


Fig. 2. Movies of the electric field amplitude for the investigated waveguide structure (Fig. 1) with varying defect height/depth h . A TE_0 mode propagating in the x direction is used as illumination. Side view through the center of the structure ($y = 0$) with a (a) linear (441 KB) and a (b) logarithmic (459 KB) color scale.

localized and even for the $h = -800$ nm notch (which completely disrupts the guiding layer) the mode re-establishes after $2.5 \mu\text{m} \approx 5\lambda_{\text{InGaAsP}} = 5\lambda/\sqrt{\epsilon_{\text{InGaAsP}}}$ because of the defect's finite lateral extension. Further, the scattering at a notch leads to a deflection of the incident mode towards the substrate at an angle which increases with the notch depth h .

Some light is also coupled out upwards into the air, which is emphasized in Fig. 2(b), where we use a logarithmic color scale. This representation evidences the mode scattering on the protrusion ($h > 0$) which produces an electric field distribution with two main lobes in the forward and the backward direction. These lobes are the forerunners of the field that would be coupled out of the structure if a long grating formed by many such elements was used. For a notch the interaction is stronger, with increasing depth h more light is coupled out and the two lobes merge into a single one.

With the logarithmic scale we can also observe remarkable interference patterns in air at a distance $z \approx 500$ nm above the InP layer. These patterns arise on both sides of the scattering element with different periodicities. They come from the interaction between the exponentially decaying electric field of the initial mode and the wave radiated in the air by the scattering element. For a quantitative analysis of this interference structure we report in Fig. 3 the electric field computed along a line 500 nm above the InP/air interface ($z = 500$ nm) for a protrusion and for a notch. Corresponding to the different propagation constants ($k_{\text{air}} = 2\pi/\lambda$ for the radiated wave and β_{TE_0} for the mode) the

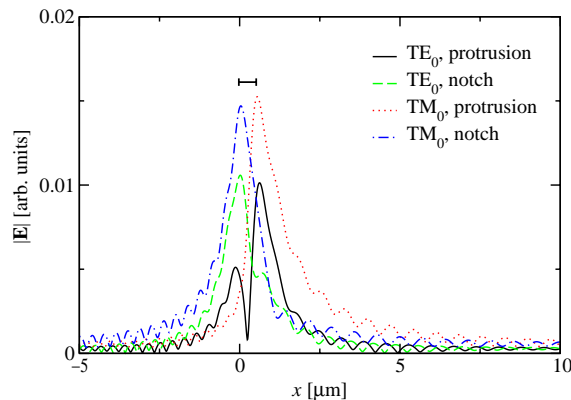


Fig. 3. Electric field amplitude in the symmetry plane ($y = 0$) 500 nm above the InP/air interface for two different defects (protrusion with $h = 100$ nm and notch with $h = -100$ nm) and two different illumination polarizations. The bar represents the extension of the defect in the x direction.

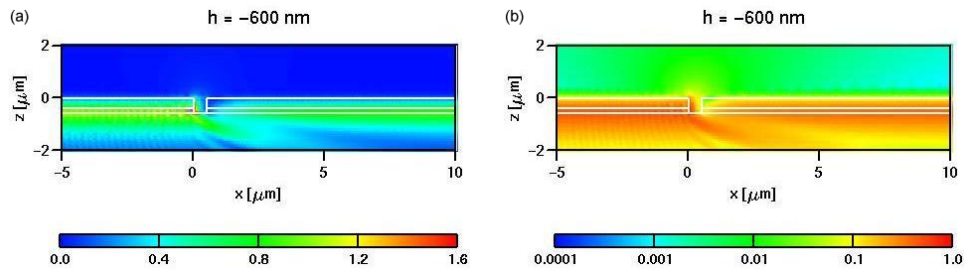


Fig. 4. Same situation as in Fig. 2 but with a TM_0 mode as illumination. The movies have a (a) linear (435 KB) and a (b) logarithmic (444 KB) color scale.

electric field amplitude is modulated with the periodicities $\Delta_{fw} = 2\pi/(\beta_{TE_0} - k_{air}) \approx 705$ nm in the forward direction and $\Delta_{bw} = 2\pi/(\beta_{TE_0} + k_{air}) \approx 369$ nm in the backward direction [6]. Our numerical results agree perfectly with these predicted numbers.

In the movies in Fig. 4 we show the same situation as in Fig. 2, but now with a TM_0 mode as excitation. With this polarization we can observe qualitatively the same features as in the TE case. However, now a protrusion also creates a field distribution with only one main lobe in forward direction. The periodicities of the interference patterns in air change only slightly since the propagation constants are similar for both modes: $\Delta_{fw} = 2\pi/(\beta_{TM_0} - k_{air}) \approx 709$ nm in forward direction and $\Delta_{bw} = 2\pi/(\beta_{TM_0} + k_{air}) \approx 370$ nm in backward direction.

Let us now study in greater detail the processes taking place inside the waveguide itself. The movies in Fig. 5 show top views of the electric field amplitude at $z = -525$ nm, i.e. inside the guiding InGaAsP layer. Again, the field distribution remains nearly homogeneous in the case of a protrusion ($h > 0$) or a shallow notch ($h \lesssim 0$). With a deeper notch the scattering increases strongly, the region behind the defect becomes depleted and a complex interference pattern arises: The interaction of the incident field and the scattered field creates in the backward direction a dense system of fringes and in forward direction a field distribution which can be interpreted as the diffraction pattern of the defect. On the left-hand side of notches deeper than $h \approx -500$ nm one also observes an interference pattern with a period larger than that mentioned above. However, this is a Moiré pattern due to the finite number of computed field points without physical significance.

Away from the defect the electric field distributions in Fig. 5 are similar for a TE_0 or a TM_0 excitation. The different polarizations can however be distinguished inside the

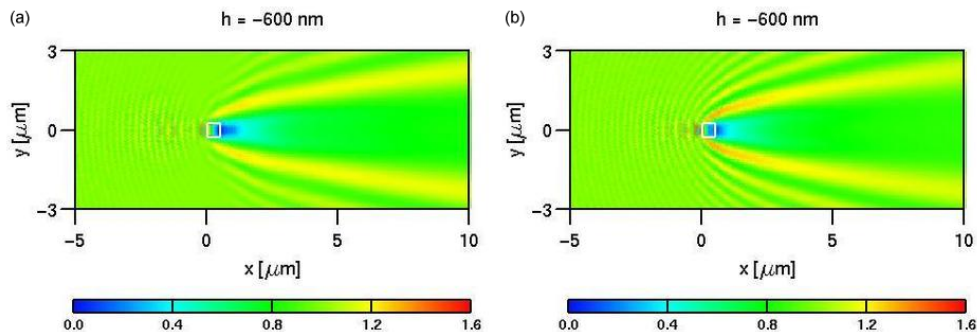


Fig. 5. Movies of the electric field amplitude in the InGaAsP layer ($z = -525$ nm) for varying defect height/depth h . Top view for a (a) TE_0 (408 KB, see Fig. 2) and a (b) TM_0 illumination (415 KB, see Fig. 4). The white box represents the extension of the defect in the xy plane.

defect: The largest fields are created at the edges normal to the electric field vector of the excitation, especially close to the front side of the defect, where the incident field is backreflected. Hence, for a TE_0 illumination with the electric field in the y direction, we observe sharp peaks at the two left inner corners when the computation plane intersects the notches [$h < -525$ nm, Fig. 5(a)]. On the other hand, for a TM_0 illumination with the electric field mainly in the z direction, the largest fields occur at the left y -directed edge of a notch. As a matter of fact, for $h = -550$ nm this edge being close to the computation plane, the corresponding figure shows a strong electric field enhancement [Fig. 5(b)].

4 Summary

In this paper we studied the scattering of a mode propagating in a planar InP/InGaAsP waveguide on a three-dimensional rectangular defect. Our simulations show in detail the dependence of the scattering strength on the vertical extension of the defect and provide insights into the local effects taking place when light is coupled out of a waveguide. However, our approach based on the Green's tensor technique is not only beneficial for the basic understanding of scattering phenomena but provides also solutions for technologically relevant problems in device development. For example, we can estimate an upper limit for the roughness in the layered waveguide system in dependence on the outcoupled energy and define process windows for the production and operation of the device.

Acknowledgements

It is a pleasure to acknowledge stimulating discussions with J. P. Kottmann and to thank B. Michel (IBM) for his support of the project. We gratefully acknowledge funding from the Swiss National Science Foundation.